metals

Article

Research on the Quality Improvement and Consumption Reduction of Iron Ore Agglomeration Based on Optimization

Mingshun Zhou [1,2,*], Desheng Zhao [3], Jiangning Zhang [4], Guang Yang [4], Enjian Hou [4], Mingxu Liu [5], Hui Zhang [1,2], Xin Jiang [6,7,*], Kai Fan [6] and Fengman Shen [6,7]

1 State Key Laboratory of Metal Material for Marine Equipment and Application, Anshan 114009, China
2 Iron and Steel Research Institute of Angang Iron and Steel Group Corporation, Anshan 114009, China
3 Iron-Making Plant, Anshan Iron and Steel Group Co., Ltd., Anshan 114000, China
4 East Anshan Sintering Plant, Anshan Iron and Steel Group Co., Ltd., Anshan 114006, China
5 Plate Research and Development Institute of Benxi Steel Co., Ltd., Benxi 117000, China
6 School of Metallurgy, Northeastern University, Shenyang 110819, China
7 Key Laboratory for Ecological Metallurgy of Multimetallic Mineral (Ministry of Education), Northeastern University, Shenyang 110819, China
* Correspondence: zms4652@163.com (M.Z.); jiangx@smm.neu.edu.cn (X.J.)

Abstract: In order to increase agglomeration production and improve its quality while reducing energy consumption, a new intelligent blending method has been established at Ansteel to optimize its sinter blends. The statistical model of the ore blending results shows that (1) a blending ratio of 47.2% Ore A and 52.8% Ore C corresponded to the best sinter yield of 72.44%. (2) From the viewpoint of sinter reducibility, sinter basicity should not be less than 1.98 when the proportion of Ore A in the blend is more than 35%. Due to the low mixing efficiency of disc pelletizers, Ansteel has therefore gone through a massive technical transformation at Sinter Plant 3 to replace its 16 existing disc pelletizers with one drum granulator. Since the installation of the drum granulator, the standard deviation has decreased from 1.517 to 0.7332 for total Fe (T.Fe) and from 0.146 to 0.0956 for basicity. In the case of the drum granulator, the standard deviation for sinter T.Fe and basicity were 0.6926 and 0.05449, respectively, as compared to 0.8902 and 0.2033 for the disc pelletizers. In addition, a single lattice method is proposed to optimize the particle-size distribution of the coke breeze to further improve sinter quality and reduce fuel consumption. The lattice method indicated that the optimum coke breeze to achieve maximum sinter tumble strength should consist of approximately 57.20%: −1 mm, 25.63%: 1–3 mm, 11.17%: 3–5 mm, and 6.00%: >5 mm particles. Given the international trend of increasing bed depth, Ansteel has successfully achieved a bed height of 1050 mm or more under its blend conditions, which typically contain 75% concentrates. Finally, some new iron ore agglomerations research is discussed.

Keywords: sinter quality and productivity; statistical model; granulation process; coke size

check for updates

Citation: Zhou, M.; Zhao, D.; Zhang, J.; Yang, G.; Hou, E.; Liu, M.; Zhang, H.; Jiang, X.; Fan, K.; Shen, F. Research on the Quality Improvement and Consumption Reduction of Iron Ore Agglomeration Based on Optimization. *Metals* **2023**, *13*, 480. https://doi.org/10.3390/met13030480

Academic Editor: Alexander McLean

Received: 29 January 2023
Revised: 22 February 2023
Accepted: 23 February 2023
Published: 26 February 2023

1. Introduction

Blast furnace ironmaking has the advantages of a good economic index, simple process, large output, and high production efficiency, which represents the major hot metal-making process in the world [1,2]. With the large-scale development of modern blast furnaces, iron ore resources are becoming increasingly scarce, which makes the raw material structure of sintering plants fluctuate greatly, and the production is extremely unstable [3]. Industry practice has demonstrated that, without high-quality sinter, modern blast furnaces are not able to run efficiently at large wind rates, high blast temperatures, and elevated PCI rates to produce premium hot metal at high productivity and low energy consumption [4–6]. Therefore, the high quality and low fuel consumption of the iron ore agglomeration process has become a hot spot and focus of research for sintering and even iron-making workers.

In order to understand the effect of average iron ore particle size on the mineralogy, productivity, and physical and metallurgical properties of sintered ores, Umadevi et al. [7] conducted pot grate sintering experiments on iron ores with different particle sizes (mean particle size of 1.22 to 3.95 mm). The sintering productivity increased with the increase in the mean particle size of iron ore due to the increase in the flame front speed (FFS) and the increase in the bed permeability at a lower sintering time. In order to improve the permeability of the sintering bed for sinter ore productivity, Matsumura et al. [8] proposed the RF-MEBIOS (return fine-mosaic embedding iron ore sintering) process, in which returned fines are added to the pellet feed as dry particles and are then loaded into the sinter. Moreover, Donskoi et al. [9] used a database of results from pilot-scale sintering experiments to develop a mathematical model for predicting the properties of different sintered ores. This model takes into account the mineralogical and textural characteristics of the iron ore used for sintering, in addition to the particle size distribution and other physical and chemical characteristics that are typically used for sinter quality prediction. However, to the best of the authors' knowledge, there are only a few reports on the relationship between a statistical model of ore blending and optimal experimental design so far.

The optimal experimental design method is a mathematical and statistical method for analyzing multifactor experiments. This method unifies the arrangement of experiments, data processing, and the accuracy of the regression equation into a whole system to study such that the regression equation (with high accuracy) can be obtained with a smaller number of experiments [10,11]. In this paper, a statistical model of rational sintering ore allocation was established using the optimal experimental design method, and a single-factor analysis of the model can resolve the influence of each iron ore species on the quality and productivity of the sintered minerals. The optimization theory is applied to derive the optimal solution on the statistical model of sintering, and the quantitative matching relationship of iron ores in obtaining the best sintering index value is derived. The optimization is carried out from different perspectives, such as improving the particle size composition of sintered ore, reduction degradation, low-temperature reduction pulverization, and sintering productivity, and different optimized ratios of various concentrates can be derived. Therefore, the model accurately reflects the regularity of sintering after the different matching of iron ores. Moreover, the Ansteel Iron and Steel Research Institute, in collaboration with the Ansteel Ironmaking plant, has, over the years, carried out a series of R&D projects to improve the sintering process. This paper summarizes some of the recent innovations and their applications, which hope to provide valuable experience for the future development and deployment of new technologies for preparing ironmaking raw materials in China.

2. Innovative Blend Optimization Technology

2.1. Background

Due to their distinct characteristics, ores behave differently at high temperatures during sintering. Therefore, the proportion of iron ore concentrates in the sinter blend will directly affect sinter production and quality [4]. In the past, the blending ratio of key concentrates in the sinter blend in Ansteel was dictated by its mining and transportation capacity, which is no longer appropriate under current raw material conditions. Since the inception of new Si reduction technology in its captive mines, both the iron grade and SiO_2 content of the self-produced concentrates have improved significantly. As a result, the grade of the sinter, as shown in Figure 1, has improved greatly. In addition, the proportion of imported iron ore fines and a lump in Ansteel has increased gradually in recent years, which has led to the corresponding changes in the high-temperature behavior of the ores in the sinter blend and, consequently, has impacted sinter productivity and quality. Therefore, fundamental research is urgently needed in Ansteel to optimize the sinter blend based on the characteristics of the raw materials to ensure ores support each other in the blend, finally achieving the sinter quality and productivity required.

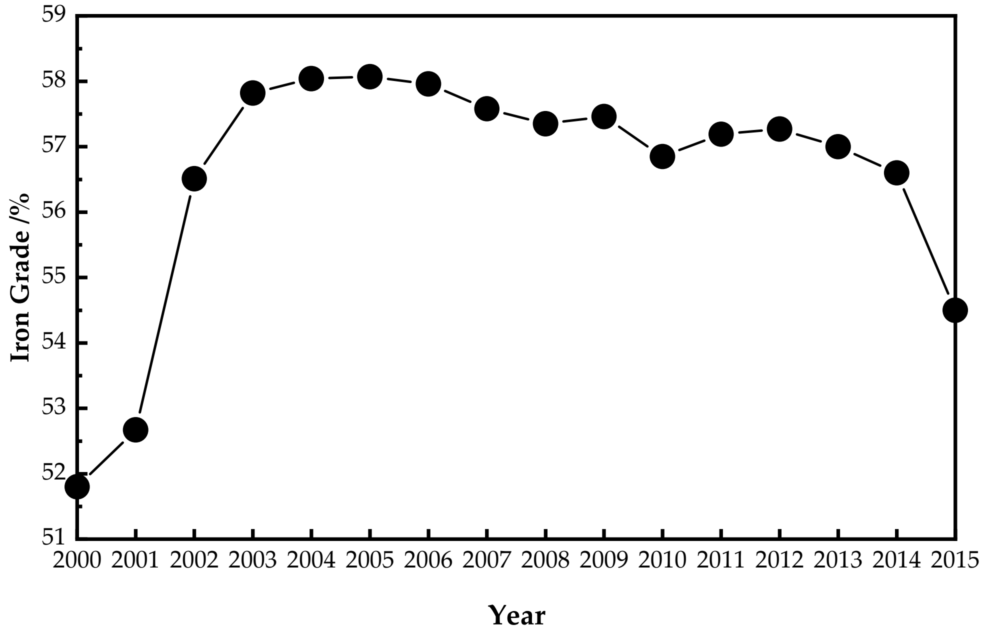

Figure 1. Variation of sinter grade in Ansteel since 2000.

2.2. Ansteel Blend Optimization Technology

The key objective of blend optimization is to select appropriate ores and their proportions in the sinter blend to ensure they support each other in the blend. Firstly, systematic studies were conducted to evaluate the fundamental sintering characteristics of iron ore concentrates from Ansteel's captive mines, including their assimilation characteristics, calcium ferrite formation ability, sinter melt fluidity, sinter matrix strength, crystal bonding ability, etc. [12]. Based on the sintering characteristics of the concentrates and their metallurgical properties, including reducibility, reduction disintegration, and the softening properties of the resultant sinters, together with ore mineralogy, the proportion of the concentrates in the blend was then optimized [13]. As a result, it was proposed that the DaCi(DC) concentrate be used predominantly in the sinter blend. In the past, it was generally believed that the Diao Jun Tai (DJT) concentrate was not suitable for pelletizing. However, using the new blend optimization technology, DJT concentrate can now be used for pellet production. This has helped the Ansteel sinter plant achieve better utilization of its resources.

Secondly, a statistical model of ore blending was established for the first time in China through optimal experimental design [14,15]. Based on the model, the influence of ores on sinter productivity and quality can therefore be evaluated through single factor analysis of variance. The empirical model of various indices is shown in Table 1.

By applying the optimization theory to the statistical model, the blending ratio of the ores that correspond to the optimum sintering performance was derived. Figure 2 shows the two-dimensional isopleth maps obtained through a single-factor analysis of the variance. The empirical model of various indices is shown in Table 3. Table 4 shows the reliability test results of a regression equation. The preliminary study on rational ore blending in laboratory sintering by using the mathematical optimization method shows that the statistical model of rational ore blending by using the orthogonal regression method has good accuracy in the statistical range. Table 5 lists the optimized sintering parameters and the corresponding blending ratios of ores required.

Table 1. Experience model of various indices.

NO	Sintering Parameters	Regression Equation	Significance *
1	Products yield %	$Y_1 = 69.00 + 0.123\ X_1 + 0.268X_2 - 0.047X_3 + 0.09X_4 - 0.151X_5 - 0.187X_1X_2 + 0.178X_1X_3 - 0.104X_1X_4 + 0.121X_1X_5 - 0.024X_2X_3 + 0.121X_2X_4 + 0.348X_2X_5 + 0.522X_3X_4 + 0.300X_3X_5 + 0.202X_4X_5 - 0.119X^2{}_1 + 0.290X^2{}_2 - 0.272X^2{}_3 - 0.234X^2{}_4 - 0.138X^2{}_5$	0.1
2	Utilization factor t/h·m^2	$Y_2 = 1.358 - 0.057X_1 - 0.0385X_2 - 0.00735X_3 - 0.056X_4 + 0.052X_5 + 0.023X_1X_2 + 0.058X_1X_3 + 0.012X_1X_4 - 0.011X_1X_5 - 0.0198X_2X_3 - 0.022X_2X_4 + 0.011X_2X_5 + 0.011X_3X_4 - 0.03X_3X_5 + 0.02X_4X_5 + 0.0057X^2{}_1 + 0.04X^2{}_2 - 0.0051X^2{}_3 + 0.038X^2{}_4 + 0.012X^2{}_5$	0.05
3	Solid fuel Consumption kg/t	$Y_3 = 45.16 + 0.258X_1 - 0.014X_2 + 0.133X_3 + 0.57X_4 - 0.75X_5 + 0.11X_1X_2 - 0.36X_1X_3 - 0.18X_1X_4 - 0.032X_1X_5 - 0.146X_2X_3 - 0.265X_2X_4 - 0.07X_2X_5 - 0.425X_3X_4 + 0.0168X_3X_5 + 0.261X_4X_5 - 0.208X^2{}_1 - 0.367X^2{}_2 + 0.003X^2{}_3 + 0.099X^2{}_4 + 0.059X^2{}_5$	0.005
4	Droop speed mm/min	$Y_4 = 18.15 - 0.824X_1 - 0.578X_2 - 0.203X_3 - 0.582X_4 + 0.633X_5 + 0.406X_1X_2 + 0.357X_1X_3 + 0.0125X_1X_4 - 0.452X_1X_5 - 0.523X_2X_3 - 0.141X_2X_4 - 0.171X_2X_5 - 0.072X_3X_4 - 0.0375X_3X_5 + 0.03X_4X_5 + 0.487X^2{}_1 + 0.734X^2{}_2 + 0.352X^2{}_3 + 1.06X^2{}_4 + 0.314X^2{}_5$	0.05
5	40~10 mm Granularity %	$Y_5 = 50.19 - 0.278X_1 + 1.415X_2 + 1.227X_3 - 0.753X_4 + 1.856X_5 + 0.139X_1X_2 - 0.383X_1X_3 + 0.042X_1X_4 - 1.196X_1X_5 - 0.568X_2X_3 - 0.278X_2X_4 + 0.021X_2X_5 + 0.27X_3X_4 - 0.386X_3X_5 - 0.70X_4X_5 - 1.59X^2{}_1 + 0.235X^2{}_2 - 0.168X^2{}_3 + 0.243X^2{}_4 + 1.41X^2{}_5$	0.1
6	10~5 mm Granularity %	$Y_6 = 8.43 + 0.239X_1 + 0.042X_2 + 0.136X_3 + 0.196X_4 - 0.685X_5 + 0.119X_1X_2 - 0.198X_1X_3 - 0.058X_1X_4 - 0.139X_1X_5 - 0.152X_2X_3 - 0.00044X_2X_4 - 0.103X_2X_5 - 0.241X_3X_4 - 0.238X_3X_5 - 0.121X_4X_5 - 0.103X^2{}_1 - 0.115X^2{}_2 + 0.284X^2{}_3 + 0.025X^2{}_4 + 0.148X^2{}_5$	0.1
7	<5mm Granularity %	$Y_7 = 5.575 + 0.09X_1 + 0.07X_2 + 0.139X_3 - 0.11X_4 - 0.037X_5 + 0.306X_1X_2 + 0.116X_1X_3 - 0.136X_1X_4 + 0.021X_1X_5 + 0.112X_2X_3 + 0.18X_2X_4 - 0.122X_2X_5 - 0.213X_3X_4 - 0.162X_3X_5 - 0.025X_4X_5 + 0.224X^2{}_1 + 0.57X^2{}_2 - 0.0033X^2{}_3 + 0.026X^2{}_4 + 0.214X^2{}_5$	0.05
8	Drum strength %	$Y_8 = 59.61 - 1.056X_1 + 0.147X_2 - 0.512X_3 - 1.235X_4 + 2.973X_5 - 0.242X_1X_2 + 0.105X_1X_3 + 0.921X_1X_4 - 0.747X_1X_5 - 0.092X_2X_3 - 0.0768X_2X_4 + 0.535X_2X_5 + 1.583X_3X_4 + 0.743X_3X_5 - 0.352X_4X_5 + 0.068X^2{}_1 - 0.475X^2{}_2 - 0.548X^2{}_3 - 0.303X^2{}_4 - 0.389X^2{}_5$	0.1
9	FeO %	$Y_9 = 11.17 + 0.158X_1 + 0.249X_2 - 0.402X_3 + 0.681X_4 - 0.101X_5 - 0.076X_1X_2 + 0.057X_1X_3 - 0.033X_1X_4 - 0.145X_1X_5 - 0.29X_2X_3 + 0.336X_2X_4 + 0.224X_2X_5 + 0.068X_3X_4 - 0.202X_3X_5 + 0.270X_4X_5 - 0.243X^2{}_1 + 0.039X^2{}_2 - 0.316X^2{}_3 + 0.434X^2{}_4 + 0.0581X^2{}_5$	0.2

Table 1. *Cont.*

NO	Sintering Parameters	Regression Equation	Significance *
10	Reduction %	$Y_{10} = 81.85 - 1.08X_1 - 0.397X_2 + 0.131X_3 - 0.719X_4 + 2.91X_5 + 0.998X_1X_2 - 0.015X_1X_3 - 0.243X_1X_4 + 1.37X_1X_5 + 0.0806X_2X_3 - 0.676X_2X_4 + 1.31X_2X_5 - 0.631X_3X_4 + 0.485X_3X_5 - 0.35X_4X_5 + 0.85X^2_1 + 0.135X^2_2 + 0.22X^2_3 + 0.42X^2_4 + 2.95X^2_5$	0.05
11	RDI (>6.3 mm) %	$Y_{11} = 70.62 - 4.12X_1 + 0.129X_2 + 0.889X_3 - 0.51X_4 + 0.578X_5 - 2.603X_1X_2 - 0.583X_1X_3 - 0.37X_1X_4 + 0.85X_1X_5 - 0.997X_2X_3 - 1.68X_2X_4 - 0.17X_2X_5 + 0.454X_3X_4 - 0.035X_3X_5 - 0.78X_4X_5 + 4.11X^2_1 + 2.267X^2_2 + 2.61X^2_3 + 2.12X^2_4 + 2.29X^2_5$	0.025
12	RDI (>3.15 mm) %	$Y_{12} = 87.14 - 1.50X_1 + 0.314X_2 + 0.651X_3 - 0.23X_4 + 0.713X_5 - 1.226X_1X_2 - 0.404X_1X_3 - 0.456X_1X_4 + 0.829X_1X_5 - 0.783X_2X_3 - 0.963X_2X_4 + 0.213X_2X_5 - 0.040X_3X_4 + 0.105X_3X_5 - 0.243X_4X_5 + 1.869X^2_1 + 0.93X^2_2 + 0.78X^2_3 + 0.893X^2_4 + 0.615X^2_5$	0.05
13	RDI (<0.5 mm) %	$Y_{13} = 2.764 + 0.336X_1 + 0.067X_2 - 0.304X_3 + 0.144X_4 - 0.412X_5 + 0.452X_1X_2 - 0.144X_1X_3 + 0.339X_1X_4 - 0.50X_1X_5 - 0.18X_2X_3 + 0.43X_2X_4 - 0.121X_2X_5 - 0.232X_3X_4 + 0.034X_3X_5 - 0.104X_4X_5 - 0.266X^2_1 - 0.141X^2_2 - 0.05X^2_3 - 0.13X^2_4 + 0.285X^2_5$	0.005

Where X_1, X_2, X_3, and X_4 refer to ores A, B, C, and D, respectively; their chemical compositions are shown in Table 2, while X_5 is the basicity of the sinter. * $a < 0.1$ is more significant, $a < 0.05$ is more significant, $a < 0.005$ is highly significant.

Table 2. Chemical composition of raw material.

Raw Material	Mass %					
	TFe	FeO	SiO_2	CaO	MgO	L OI
Ore A	67.50	16.70	2.80	<0.15	0.55	−0.57
Ore B	67.15	17.24	4.85	<0.15	0.30	−0.84
Ore C	68.26	29.09	5.00	<0.15	0.30	−2.68
Ore D	66.73	28.74	7.10	<0.15	0.35	−2.26

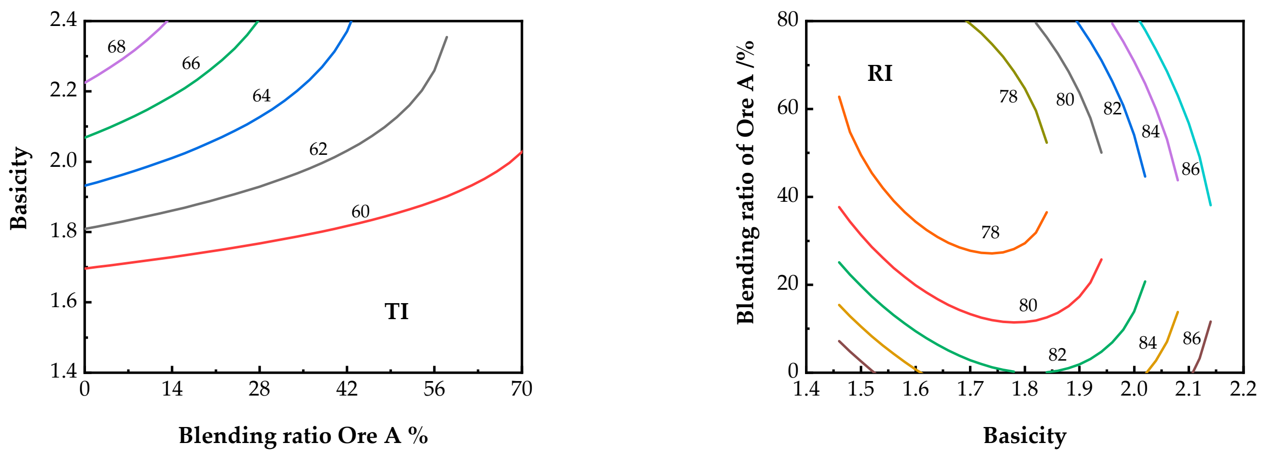

(**a**) (**b**)

Figure 2. Two-dimensional isopleth maps (**a**) ISO tumble index; (**b**) ISO reducibility.

Table 3. Variance analysis of combination design.

Index	Quadratic Sum	Degree of Freedom	Mean Sum of Square	$F = (S_r/f_r)/(S_e/f_e)$	Significance
Y_1	$S_t = 16.75$, $S_r = 15.46$, $S_e = 1.30$	$f_t = 26$, $f_r = 20$ $f_e = 6$	$S_r/f_r = 0.773$, $S_e/f_e = 0.217$	3.56	$F, > F_{0.10}(20,6) = 2.84$
Y_2	$S_t = 0.393$, $S_r = 0.371$, $S_e = 0.022$	$f_t = 26$, $f_r = 20$ $f_e = 6$	$S_r/f_r = 0.0186$, $S_e/f_e = 0.0037$	5.03	$F, > F_{0.05}(20,6) = 3.87$
Y_3	$S_t = 31.54$, $S_r = 30.77$, $S_e = 0.77$	$f_t = 26$, $f_r = 20$ $f_e = 6$	$S_r/f_r = 1.5385$, $S_e/f_e = 0.1284$	11.98	$F, > F_{0.005}(20,6) = 9.59$
Y_4	$S_t = 80.08$, $S_r = 75.00$, $S_e = 5.088$	$f_t = 26$, $f_r = 20$ $f_e = 6$	$S_r/f_r = 3.75$, $S_e/f_e = 0.8480$	4.42	$F, > F_{0.05}(20,6) = 3.87$
Y_5	$S_t = 277.2$, $S_r = 254.6$, $S_e = 22.55$	$f_t = 26$, $f_r = 20$ $f_e = 6$	$S_r/f_r = 12.73$, $S_e/f_e = 3.7584$	3.39	$F, > F_{0.10}(20,6) = 2.84$
Y_6	$S_t = 18.95$, $S_r = 17.51$, $S_e = 1.45$	$f_t = 26$, $f_r = 20$ $f_e = 6$	$S_r/f_r = 0.8755$, $S_e/f_e = 0.2417$	3.62	$F, > F_{0.10}(20,6) = 2.84$
Y_7	$S_t = 10.64$, $S_r = 9.93$, $S_e = 0.709$	$f_t = 26$, $f_r = 20$ $f_e = 6$	$S_r/f_r = 0.4965$, $S_e/f_e = 0.1182$	4.20	$F, > F_{0.05}(20,6) = 3.87$
Y_8	$S_t = 362.35$, $S_r = 332.7$, $S_e = 29.61$	$f_t = 26$, $f_r = 20$ $f_e = 6$	$S_r/f_r = 16.635$, $S_e/f_e = 4.935$	3.37	$F, > F_{0.10}(20,6) = 2.84$
Y_9	$S_t = 53.13$, $S_r = 46.69$, $S_e = 6.44$	$f_t = 26$, $f_r = 20$ $f_e = 6$	$S_r/f_r = 2.3345$, $S_e/f_e = 1.0734$	2.17	$F, > F_{0.20}(20,6) = 2.0$
Y_{10}	$S_t = 451.59$, $S_r = 419.8$, $S_e = 31.79$	$f_t = 26$, $f_r = 20$ $f_e = 6$	$S_r/f_r = 20.99$, $S_e/f_e = 5.2984$	3.96	$F, > F_{0.05}(20,6) = 3.87$
Y_{11}	$S_t = 1077.4$, $S_r = 1026.4$, $S_e = 50.95$	$f_t = 26$, $f_r = 20$ $f_e = 6$	$S_r/f_r = 51.32$, $S_e/f_e = 8.4917$	6.04	$F, > F_{0.025}(20,6) = 5.17$
Y_{12}	$S_t = 222.5$, $S_r = 206.98$, $S_e = 15.52$	$f_t = 26$, $f_r = 20$, $f_e = 6$	$S_r/f_r = 10.349$, $S_e/f_e = 2.5867$	4.00	$F, > F_{0.05}(20,6) = 3.87$
Y_{13}	$S_t = 25.39$, $S_r = 24.74$, $S_e = 0.65$	$f_t = 26$, $f_r = 20$, $f_e = 6$	$S_r/f_r = 1.237$, $S_e/f_e = 0.1084$	11.41	$F, > F_{0.005}(20,6) = 9.59$

As seen in Table 5, a blend consisting of 47.2% Ore A and 52.8% Ore C shows the best sinter yield of 72.44%. In Figure 2, in the basicity range tested, sinter tumble strength decreases as the proportion of Ore A in the blend increases; however, from the viewpoint of sinter reducibility, sinter basicity should not be less than 1.98 when the proportion of Ore A in the blend is more than 35%. Hence the optimum blending ratio can be determined depending on the intended objectives. However, in actual production, apart from the ore characteristics, the availability of the ores, the capacity of charge bins, the layout of the sinter plant, and other constraints also need to be carefully considered [7].

After adopting the proposed sinter blend, Sinter Plant No 2 increased its productivity by 0.07 t/m^2h and reduced its fuel rate by 0.9 kg/t and returns ratio by 0.37%. This suggests that the ore proportioning scheme developed can achieve higher economic benefits and higher quality sinter. This has demonstrated that a good blending philosophy will not only enhance economic benefits but also improve sinter quality [16].

Table 4. Results of regression equation reliability check.

Products Yield %		**Drum Strength %**		**Utilization Factor t/h·m^2**		**Solid Fuel Consumption kg/t**		**Granularity 10–5 mm%**		**Reduction %**	
Calculated value	Experimental value	Calculated value	Experimental value	Calculated value	Experimental value	Calculated value	Experimental value	Calculated value	Experimental value	Calculated value	Experimental value
69.12	69.46	63.42	63.56	1.460	1.446	43.01	42.91	7.28	7.78	87.97	88.01

Table 5. Optimized sintering parameters and the required corresponding ratios.

No	Sintering Parameters	Optimum Value	Corresponding Ore Blending ratio				Worst Value	Corresponding Ore Blending Ratio			
			A	B	C	D		A	B	C	D
1	Products yield, %	72.4	47.2		52.8		64.2		28.0	32.3	39.7
2	Utilization factor, t/h·m^2	2.0				100.0	0.9	82.2	17.7		
3	Solid fuel Consumption, kg/t	38.4		41.2		58.7	48.5	82.2	17.7		
4	Droop speed, mm/min	29.2		28.2	32.4	39.4	15.4	39.3	12.5	29.4	18.9
5	40–10 mm Granularity, %	64.1	26.7			73.3	37.5		51.1		48.9
6	10–5 mm Granularity, %	5.9	57.3		42.7		12.2	100.0			
7	<5 mm Granularity, %							34.8	7.3	25.9	32.0
8	Drum strength, %	75.4				100.0	43.6	37.6		27.9	34.5
9	FeO, %	5.9	37.4		28.2	34.4	15.3	100.0			
10	Reduction, %	91.0	37.4		28.2	34.4	73.7	57.0		43.0	
11	RDI (>6.3 mm), %	86.0				100.0	59.7	46.2	14.8	17.0	22.0
12	RDI (>3.15mm), %	93.0			44.8	55.3	81.5	66.5		33.5	
13	RDI (<0.5 mm), %	2.1	40.9	27.0	31.1		10.3	100.0			

3. Rectification of Improper Granulation Process

At the beginning of the process, the Ansteel Sinter Plant 3 experienced significant variations in sinter quality, which led to a considerable increase in the blast furnace fuel rate and hot metal cost. After carrying out extensive experiments and data analysis at the Ansteel Research Institute, it was found that the inferior mixing efficiency of the disc pelletizing process used in Sinter Plant 3 was responsible for the observed variation in sinter quality [17]. For the first time in China, Ansteel proposed to replace the disc pelletizer with a drum granulator. The drum granulator has a diameter, length, rotation speed, and tilt angle of 5100 mm, 24,500 mm, 5.5 r/min, and 1.6°, respectively. The disc granulator has a diameter, height, and tilt angle of 6000 mm, 600 mm, and 50°, respectively. As a result, 16-disc pelletizers in Sinter Plant 3 were replaced with one drum granulator as part of a technological transformation program. The results from the plant operation were as follows:

- When compared with the disc pelletizers, the drum granulator showed better mixing efficiency. The mixture after the drum granulator was found to be more uniform and stable in chemical composition and basicity. Since the installation of the drum granulator, the standard deviation has decreased from 1.517 to 0.7332 for total Fe (T.Fe) and from 0.146 to 0.0956 for basicity;
- When compared with the sinter from Sinter Plant 3, where the disk palletizers were previously used, the chemical composition and basicity of the sinter obtained from Sinter Plant 2, in which a drum granulator was used, were more stable and less scattered. The standard deviation for sinter T.Fe and basicity were 0.6926 and 0.05449, respectively, in the case of the drum granulator and 0.8902 and 0.2033 in the case of the disc palletizers;
- Since the introduction of a drum granulator to replace the 16 existing disc pelletizers for secondary mixing, Sinter Plant 3 has experienced very stable operation with a marked improvement in its sintering performance. The sinter pot test conditions are shown in Table 6. Table 7 compares the key sintering indices before and after the installation of the drum granulator. As shown in Table 7, the sinter chemistry, as evidenced by basicity, T.Fe, and FeO [18,19], was more stable and consistent through the test period than the base case. There was also a slight improvement in sintering productivity and a considerable reduction in fuel consumption (4 kg/t).

Table 6. Sintering condition of pot test.

Bed height mm	600
Ignition temperature °C	1050
Ignition time min	2
Ignition suction value Pa	8820
Extraction negative pressure Pa	10,780

Table 7. Key sintering indices before and after installation of the drum granulator.

Mean Value	The Yield of First-Grade Products %	Variation in Sintering Basicity %	Coefficient of Stabilization of FeO %	Coefficient of Stabilization of TFe %	Productivity t/h·m^2	Solid Fuel Consumption kg/t
Base	84.8	89.2	94.9	91.7	1.0	42
Test	91.8	95.5	95.9	94.6	1.1	38
Difference	+7.0	+6.3	+0.95	+2.9	+0.08	−4

In conclusion, the experience from the No 3 Sinter Plant has fully demonstrated that the drum granulator is the better option for even mixing. Therefore, the disc palletizers in existing sintering plants should be replaced.

Optimization of Fuel Particle Size

The addition level, granularity, and combustion characteristics of the fuel used will directly affect the distribution of heat and temperature across the sintering bed, the thickness and permeability of the flame front, and the gases generated during sintering. When the type and addition level of fuel is fixed, the particle size becomes a decisive factor in the sintering process. The particle size of solid fuel will change the combustion rate of carbon particles and, consequently, directly affect the formation of sinter phases during the sintering process. Therefore, based on practical production conditions, Ansteel has carried out laboratory studies to optimize the grain size of the coke breeze [20].

In the laboratory experiment, coke breeze was divided into four different size fractions: <1 mm, 1–3 mm, 3–5 mm, and >5 mm, and Z_1, Z_2, Z_3, and Z_4 were the normalized addition level of the fractions from fine to coarse sizes. The test work was carried out according to an experimental design using the single lattice method. The test results were then evaluated through regression analysis to establish quantitative relationships between the key sintering parameters and coke breeze size fractions. For example, the sinter tumble strength Y can be expressed by the following regression model:

$$\begin{gathered} Y = 60.48Z_1 + 57.76Z_2 + 45.09Z_3 + 38.28Z_4 + 13.44Z_1 \times Z_2 + 34.26Z_1 \times Z_3 \\ + 50.92Z_1 \times Z_4 + 27.58Z_2 \times Z_3 + 38Z_2 \times Z_4 + 3.86Z_3 \times Z_4 \end{gathered} \tag{1}$$

In order to validate the above equation, it was solved to find the optimum size distribution of the coke breeze required to achieve the maximum sinter strength. Table 8 shows the comparison between the optimum coke size distribution derived from Equation (1) and the coke breeze currently used in sinter plants. Clearly, the size distribution of the coke breeze used in sinter plants was not optimum. Sinter pot tests were carried out using both coke breezes to validate Equation (1), and the test results are summarized in Table 9. As shown in Table 9, compared with the sinter plant coke breeze, the size-optimized coke breeze has improved the sinter tumble strength, yield, and particle size distribution and reduced the fuel consumption while maintaining the vertical sintering speed and sintering productivity [21].

Table 8. Particle size distribution of the sinter plant coke breeze and the size-optimized coke breeze.

Size Fraction	<1 mm	1–3 mm	3–5 mm	>5 mm
Coke breeze used in sinter plants	35.4	50.0	8.2	6.4
Size-optimized coke breeze to achieve the maximum tumble strength	57.2	25.6	11.2	6.0

Table 9. Sinter pot test results using coke breezes of different size distributions.

	Tumble Strength %	Sintering Productivity t/(h·m^2)	Fuel Rate kg/t	Sinter Yield %	Vertical Sintering Speed mm/min	Sinter Particle Size %	
						40–10 mm	<5 mm
Sinter plant coke breeze	63.1	1.5	57.3	62.8	22.2	56.5	19.0
Size-optimized coke breeze	64.6	1.5	56.6	64.5	21.6	58.6	18.3
Variation	+1.5	−0.013	−0.7	+1.7	−0.6	+2.16	−0.79

Therefore, the optimum coke breeze to achieve maximum sinter tumble strength should consist of approximately 57.20%: −1 mm, 25.63%: 1–3 mm, 11.17%: 3–5 mm, and 6.00%: >5 mm particles, as evidenced in Table 8. Similarly, the size distribution of coke breeze can also be optimized to maximize other sintering parameters. It is, therefore, possible to satisfy various sintering parameters depending on the intended objectives through the optimization of the coke breeze size distribution. This approach has provided useful guidance to improve sinter production and quality while reducing solid fuel consumption [4].

4. Optimization of Process Variables and Sinter Composition

Optimization of Process Variables

The sintering process can be described by both mechanistic and statistical methods. The former is often derived from complex physical or mathematical equations based on many assumptions on the model parameters; hence, it has very limited success in predicting actual plant data. On the other hand, the latter is based on Mathematical Statistics and has been widely used for modeling phenomena in the metallurgical industry. This method has proved effective and easy to arrive at a solution. Therefore, the latter method was used in the present study.

In the statistical model, the target variables were selected based on production needs, including sintering productivity, sinter yield, tumble strength, vertical sintering speed, fuel rate, % −40 + 10 mm sinter, and % −5 mm sinter. Then it is important to find statistical relationships between the target variables and the blend composition and process variables, from which an optimum solution can be found through optimization, finally achieving the best overall sintering performance through blend optimization.

If Y represents a set of optimized target variables, the following equations can be written:

$$Y_1(\text{sintering productivity}) = \mathrm{E}(X_1,\ X_2, \ldots,\ X_i) \tag{2}$$

$$Y_2(\text{product yield}) = \mathrm{F}(X_1,\ X_2, \ldots,\ X_i) \tag{3}$$

$$Y_3(\text{tumble strength}) = \mathrm{G}(X_1,\ X_2, \ldots,\ X_i) \tag{4}$$

$$Y_4(\text{vertical sintering speed}) = \mathrm{H}(X_1,\ X_2, \ldots,\ X_i) \tag{5}$$

$$Y_5(\text{fuel rate}) = \mathrm{I}(X_1,\ X_2, \ldots,\ X_i) \tag{6}$$

$$Y_6(\%10\text{–}40\ \text{mm}) = \mathrm{Z}(X_1,\ X_2, \ldots,\ X_i) \tag{7}$$

$$Y_7(< \% - 5\ \text{mm}) = \mathrm{K}(X_1,\ X_2, \ldots,\ X_i) \tag{8}$$

where i is the number of independent variables utilized. If some of the independent variables are fixed, then the influence of the other variables on sintering productivity and sinter quality can be quantified. These nonlinear equations are solved simultaneously by applying certain constraints, such as tumble strength (Y_3) > 60%, sintering productivity (Y_1) > 1.25 t/h·m^2, etc., to obtain various optimum ore blends depending on the intended objectives and the optimum ore blend to achieve the overall sintering performance.

In this study, the sinter basicity, MgO content, and bed height were fixed at 2.05, 2.5%, and 670 mm [22,23], respectively. Based on the orthogonal experimental design method, a total of 27 sinter pot tests were carried out. Duplicate tests were conducted for each sinter pot test to ensure the repeatability of the experimental results, and the average values of the duplicate tests were used for quadratic regression. Figure 3 shows the isopleth diagram of sinter tumble strength.

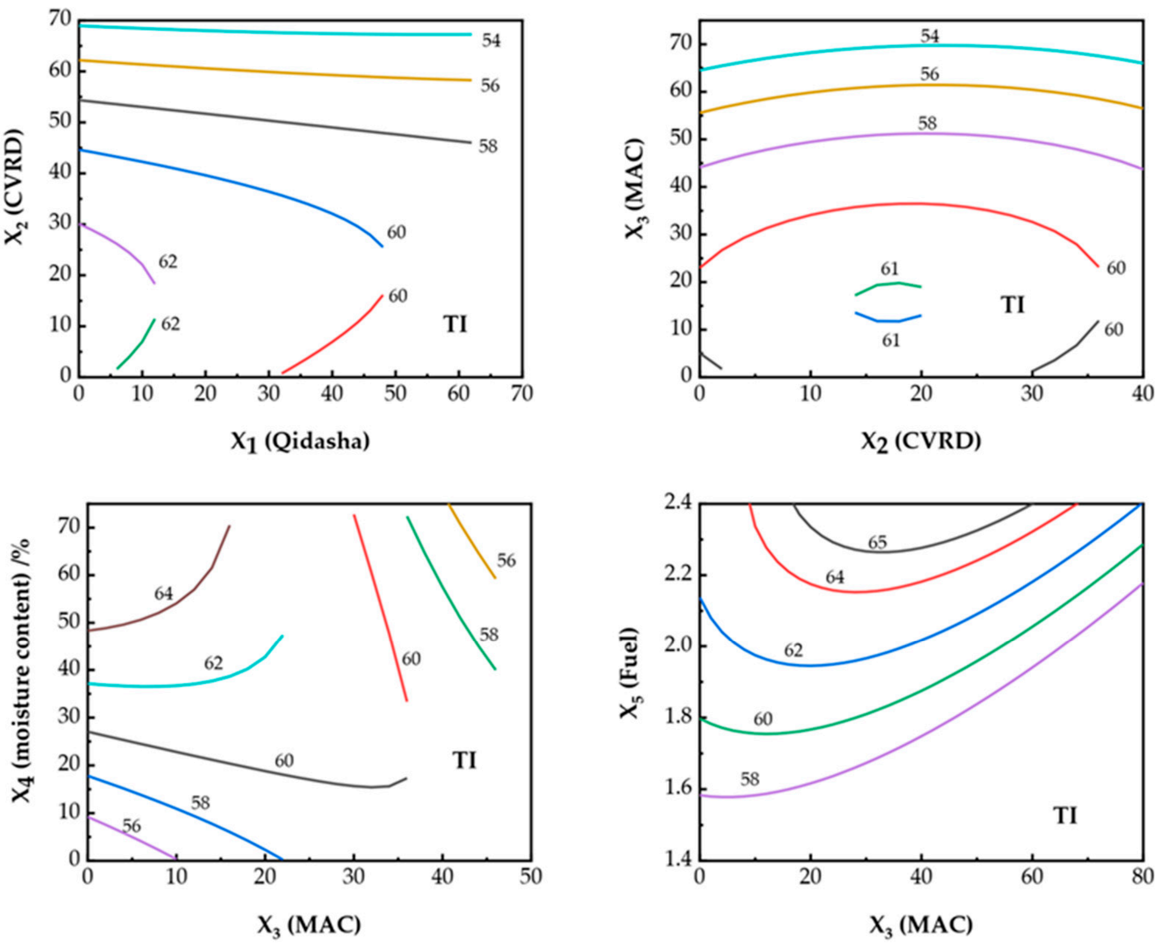

Figure 3. Isopleth maps of sinter tumble strength.

According to the current raw material conditions, the independent variables in Equations (2)–(8) were selected as follows:

$$X_1 :\rightarrow \text{\%Qidashan concentrate in the blend}$$
$$X_2 :\rightarrow \text{\%CVRD ore fine in the blend}$$
$$X_3 :\rightarrow \text{\%MAC fine in the blend}$$
$$X_4 :\rightarrow \text{\%moisture in the sinter mixture}$$
$$X_5 :\rightarrow \text{\%coke in the sinter mixture}$$

It can be seen from Figure 3 that the mix moisture content had the most impact on the sinter tumble strength, followed by % coke breeze, %CVRD fines, %Qidashan concentrate, and %MAC fines. After analyzing the quadratic coefficients in Equation (4), the effect of %Qidashan concentrate, %coke breeze, and %MAC fines on the sinter tumble strength, Y_3, was found to show an extremum. Therefore, to achieve the maximum sinter strength, these variables, including %CVRD fines, must be targeted in the region where the tumble strength shows a maximum. Constrained optimization of this aspect was used to find the optimum blend composition to maximize both the sintering productivity and sinter quality. It was found that the influence of Qidashan concentrates on the sinter tumble strength could not be ignored when the coke addiction was low. The coke addition should not be less than 5.1% when Qidashan concentrates in the blend are more than 30%. Marked interaction was observed between MAC fines and coke breeze, and the maximum tumble strength was achieved at 8% MAC fines and 5.2% coke breeze. A minimum in tumble strength was observed at 15% MAC fines and 20% Brazilian CVRD fines, which should be avoided in actual production.

5. Outlook of Agglomerations

While Ansteel has, over the years, conducted extensive fundamental work and accumulated practical experience in ironmaking raw materials, more work is still needed to address increasingly challenging raw material conditions and further reduce raw material costs [17,18]. Some of the key research focuses are summarized below.

5.1. Development of an Evaluation System for Iron Ore Sinter Fines

A sinter database was established by the Ansteel Iron and Steel Research Institute ironmaking raw material research group for ore blending. From the database, various inquiries can be made to obtain the sinter characteristics and cost information for the iron ores used by Ansteel. It can also automatically generate the optimum blend based on the constraints applied and forecast the blended cost. Further work will be focused on developing an evaluation system for iron ores [24], which can be used for both blend optimization and the purchase of iron ores. When raw material conditions change, the evaluation system will enable Ansteel to propose alternative ore blends to meet sinter quality requirements at the acceptable raw material cost.

5.2. Development of New Innovative Sintering Technologies

Based on the burden structure and metallurgical properties required by the blast furnace, composite basicity sintering technology was proposed to simplify the blast furnace burden material [25,26]. Unlike the traditional approach that only pays attention to the permeability of the sinter bed, it is focused more on the granularity, mineral, and chemical composition distribution across the sinter bed to effectively control the sintered structure and quality to meet the demanding blast furnace process. The proposed "pellet-sinter" concept will change the conventional blast furnace burden structure and can greatly decrease the ironmaking raw material cost. In the meantime, Ansteel is paying close attention to new emerging sintering technologies, such as oxygen-enriched sintering, gas-fuel-injected sintering, etc.

5.3. Development of Double-Layer Sintering New Technology with Super-Thick Layer

In order to adopt deep bed sintering technology to further increase sinter production, a new sintering technology with a double layer was proposed by the Ansteel Iron and Steel Research Institute [27,28]. The feasibility of the new technology has been confirmed by laboratory-scale tests and plant trials. The new technology enables the production of high-quality sinter from sinter blends containing more than 75% concentrate at a bed depth of 1050 mm. The application of this technology will no doubt create enormous economic benefits for Ansteel.

6. Conclusions

Agglomeration quality, as one of the key blast furnace burden material factors, is very important to the blast furnace ironmaking process. In order to increase agglomeration production and improve its quality while reducing energy consumption, a new intelligent blending method was established at Ansteel to optimize its sinter blends. The main findings can be summarized as follows:

(1) By applying the optimization theory to the statistical model, the blending ratio of 47.2% Ore A and 52.8% Ore C corresponded to the best sinter yield of 72.44%. Besides, from the viewpoint of sinter reducibility, sinter basicity should not be less than 1.98 when the proportion of Ore A in the blend is more than 35%. After adopting the proposed sinter blend, Sinter Plant No 2 increased its productivity by 0.07 t/m^2h and reduced its fuel rate by 0.9 kg/t and returns ratio by 0.37%;

(2) Since the installation of the drum granulator, the standard deviation has decreased from 1.517 to 0.7332 for total Fe (T.Fe) and from 0.146 to 0.0956 for basicity. Moreover, the standard deviation for sinter T.Fe and basicity were 0.6926 and 0.05449, respectively, in the case of the drum granulator, as compared with 0.8902 and 0.2033 for the disc palletizers. A drum granulator was used for more stability and less scattering;

(3) Using the single-lattice method, the optimum coke breeze to achieve maximum sinter tumble strength should consist of approximately 57.20%: -1 mm, 25.63%: 1–3 mm, 11.17%: 3–5 mm, and 6.00%: >5 mm particles;

(4) After analyzing the quadratic coefficients in Equation (4), the coke addition should not be less than 5.1% when the Qidashan concentrate in the blend constitutes more than 30%. Marked interaction was observed between MAC fines and coke breeze, and the maximum tumble strength was achieved at 8% MAC fines and 5.2% coke breeze. A minimum in tumble strength was observed at 15%.

Author Contributions: Conceptualization, M.Z.; methodology, X.J.; investigation, D.Z., J.Z., G.Y. and E.H.; supervision, M.L., H.Z., K.F. and F.S. All authors have read and agreed to the published version of the manuscript.

Funding: Financial support by the National Natural Science Foundation of China (NSFC 52074074, NSFC 51974073), the National Key Research and Development Program of China (Grant No. 2021YFC2902401), and the Xingliao Talent Project (XLYC2007152) are much appreciated.

Data Availability Statement: The data presented in this work are available from the corresponding author upon reasonable request.

Conflicts of Interest: The authors declare that they have no known competing financial interests or personal relationships that could have appeared to influence the work reported in this paper.

References

1. Ahmed, H. New trends in the application of carbon-bearing materials in blast furnace iron-making. *Minerals* **2018**, *8*, 561. [CrossRef]
2. Lu, Z.; Gu, H.; Chen, L.; Liu, D.; Yang, Y.; McLean, A. A review of blast furnace iron-making at Baosteel facilities. *Ironmak. Steelmak.* **2019**, *46*, 618–624. [CrossRef]
3. Smith, M.P. Blast furnace ironmaking—A view on future developments. *Procedia Eng.* **2017**, *174*, 19–28. [CrossRef]
4. Lu, L. Important iron ore characteristics and their impacts on sinter quality—A review. *Min. Metall. Explor.* **2015**, *32*, 88–96. [CrossRef]
5. Kieush, L.; Koveria, A.; Boyko, M.; Yaholnyk, M.; Hrubiak, A.; Molchanov, L.; Moklyak, V. Influence of biocoke on iron ore sintering performance and strength properties of sinter. *Min. Min. Depos.* **2022**, *16*, 55–63. [CrossRef]
6. Kieush, L.; Koveria, A.; Schenk, J.; Rysbekov, K.; Lozynskyi, V.; Zheng, H.; Matayev, A. Investigation into the Effect of Multi-Component Coal Blends on Properties of Metallurgical Coke via Petrographic Analysis under Industrial Conditions. *Sustainability* **2022**, *14*, 9947. [CrossRef]
7. Umadevi, T.; Brahmacharyulu, A.; Roy, A.K.; Mahapatra, P.C.; Prabhu, M.; Ranjan, M. Influence of iron ore fines feed size on microstructure, productivity and quality of iron ore sinter. *ISIJ Int.* **2011**, *51*, 922–929. [CrossRef]
8. Matsumura, M.; Yamaguchi, Y.; Hara, M.; Kamijo, C.; Kawaguchi, T.; Nakagawa, Y. Improvement of sinter productivity by adding return fine on raw materials after granulation stage. *ISIJ Int.* **2013**, *53*, 34–40. [CrossRef]

9. Donskoi, E.; Manuel, J.R.; Clout, J.M.; Zhang, Y. Mathematical modeling and optimization of iron ore sinter properties. *Isr. J. Chem.* **2007**, *47*, 373–379. [CrossRef]
10. Zhou, M.S.; Liu, W.S.; Dou, L.W.; Li, Y.R.; Zhai, L.W. Study on rational use of iron ore concentrate produced by Angang Iron and Steel Group Co. itself. *Iron Steel* **2006**, *41*, 11–15.
11. Zhou, M.S.; Zhai, L.W.; Li, Y.R. Laboratory study on reasonable MgO content in the sinter of Anshan Iron and Steel Group Co. *Sinter. Pelletizing* **2005**, *30*, 1–4.
12. Wang, L.; Jiang, X.; Wang, Q.Y.; Ai, M.X.; Yin, X.W.; Liu, J.T.; Shen, F.M. Investigation on segregation granulation by fuel and flux in coating. *Minerals* **2023**, *13*, 134. [CrossRef]
13. Jiang, X.; Zhao, J.D.; Wang, L.; An, H.W.; Gao, Q.J.; Zheng, H.Y.; Shen, F.M. Effects of liquidus temperature and liquid amount on the fluidity of bonding phase and strength of sinter. *ISIJ Int.* **2021**, *61*, 86–92. [CrossRef]
14. He, H.Y.; Wang, Q.X.; Zeng, X.N. Effect of MgO content on BF slag viscosity. *J. Iron Steel Res. Int.* **2002**, *25*, 340–341.
15. Yang, S.P.; Liu, H.; Ju, J.T.; Guo, Q.H. Experimental research on the effect of MgO on viscosity of BF slag. *Metall. Collect.* **2008**, *3*, 11–13.
16. Zhang, Y.Z.; Geng, M.S.; Xiang, L.; Yin, J.C.; Tao, W. The influence of MgO and basicity on the viscosity of BF slag. *J. Mater. Metall.* **2005**, *4*, 253–255.
17. Lu, Y.; Wu, S.; Niu, L.; Liu, Z.; Zhou, H.; Hong, Z.; Song, S. Treatment of vanadium–titanium magnetite based on composite agglomeration process. *Ironmak. Steelmak.* **2021**, *48*, 477–482. [CrossRef]
18. Jiang, X.; Zhang, H.Y.; Zheng, H.Y.; Gao, Q.J.; Shen, F.M. Three-segment control theory of MgO/Al_2O_3 ratio based on viscosity experiments and phase diagram analyses at 1500 °C. *J. Iron Steel Res. Int.* **2020**, *27*, 624–630. [CrossRef]
19. Jiang, X.; An, H.W.; Han, H.S.; Ding, X.; Li, L.S.; Shen, F.M. Reaction characteristics between sinter and serpentine. *Metall. Mater. Trans. B* **2020**, *51*, 937–944. [CrossRef]
20. Machida, S.; Takahide, H.; Oyama, N.; Sato, H.; Takeda, K.; Yamashita, K.; Tamura, K. Optimization of Coke Breeze Segregation in Sintering Bed under High Pisolite Ore Ratio. *ISIJ Int.* **2009**, *49*, 667–675. [CrossRef]
21. Loo, C.E.; Leung, W. Factors Influencing the Bonding Phase Structure of Iron Ore Sinters. *ISIJ Int.* **2007**, *43*, 1393–1402. [CrossRef]
22. Jiang, X.; Yu, J.X.; Wang, L.; He, T.Y.; Zheng, H.Y.; Gao, Q.J.; Shen, F.M. Fundamentals of the reduction of SFC in CO/CO_2 gas at 1000 °C. *ISIJ Int.* **2020**, *60*, 2191–2198. [CrossRef]
23. Jiang, X.; Yu, J.X.; Wang, L.; Xiang, D.W.; Gao, Q.J.; Zheng, H.Y.; Shen, F.M. Distribution of reformed coke oven gas in shaft furnace. *J. Iron Steel Res. Int.* **2020**, *27*, 1382–1390. [CrossRef]
24. Zhou, Y.L.; Jiang, X.; Wang, X.A.; Wang, L.; He, L.; Shen, F.M. Optimizing Iron Ore Proportion Aimed for Low Cost by Linear Programming Method. *Metall. Mater. Trans. B* **2022**, *53*, 4075–4086. [CrossRef]
25. Cheng, Z.; Yang, J.; Zhou, L.; Liu, Y.; Wang, Q. Sinter strength evaluation using process parameters under different conditions in iron ore sintering process. *Appl. Therm. Eng.* **2016**, *105*, 894–904. [CrossRef]
26. Jiang, T.; Li, G.H.; Wang, H.T.; Zhang, K.C.; Zhang, Y.B. Composite agglomeration process (CAP) for preparing blast furnace burden. *Ironmak. Steelmak.* **2010**, *37*, 1–7. [CrossRef]
27. Jiang, T.; Yu, Z.; Peng, Z.; Rao, M.; Zhang, Y.; Li, G. Preparation of BF Burden from Titanomagnetite Concentrate by Composite Agglomeration Process. *ISIJ Int.* **2015**, *55*, 1599–1607. [CrossRef]
28. Liu, J.; Zhou, M.; Wu, F.; Zhang, H.; Xu, L.; Zhai, L.; Gao, W.; Zhong, Q. Study of the Double-Layer Sintering Process with Stand-Support. *Metals* **2022**, *12*, 629. [CrossRef]